JAMCM Journal of Applied Mathematics and Computational Mechanics 2023, 22(1), 70-81
www.amcm.pcz.pl p-ISSN 2299-9965
DOI: 10.17512/jamcm.2023.1.06 e-ISSN 2353-0588

FREE VIBRATION OF A TWO-STAGE HYDRAULIC CYLINDER

Sebastian Uzny, Franciszek Adamek, Łukasz Kutrowski

Department of Mechanics and Fundamentals of Machine Design
Czestochowa University of Technology
Czestochowa, Poland
uzny@imipkm.pcz.pl, franciszek.adamek@pcz.pl, lukasz.kutrowski@pcz.pl

Received: 27 April 2022; Accepted: 28 August 2022

Abstract. This paper presents the problem of natural vibration of a two-stage hydraulic cylinder subjected to Euler compression load. The considered hydraulic cylinder is freely supported at both of its ends. The linear vibration problem of the telescopic hydraulic cylinder is based on the kinetic stability criterion using Hamilton's principle and the Bernoulli-Euler theory. The stiffness of the guide and sealing elements between successive stages of the hydraulic cylinder were considered in this paper. These stiffnesses were modelled using translational and rotational springs. The effects of cylinder wall thickness, piston rod diameter, and thickness of guiding and sealing elements on the natural vibration of the system were analysed. Results are presented in the form of characteristic curves on the plane load – natural frequency with different parameters characterizing the considered hydraulic cylinder.

MSC 2010: *65P99, 70J25, 70J30, 70H25*
Keywords: *hydraulic cylinder, free vibration, Euler load*

1. Introduction

Hydraulic cylinders are among the systems that are used in many industries. Due to very high longitudinal forces, they are vulnerable to damage. Hydraulic cylinders are highly responsible elements of mechanical structures, whose destruction may have very serious consequences, both material and resulting from the loss of people's health and lives. Damage to a hydraulic cylinder can result from many factors. The most exposed components of the hydraulic cylinders are the guiding and sealing elements. Repair of these parts usually means replacement of the worn-out elements with new ones and the inspection of the inner surfaces of the cylinder and piston rod for corrosion. When repairing a hydraulic cylinder, other visible mechanical damage that may lead to faster wear of the sealing and guiding rings must also be taken into account. During the design of hydraulic cylinders, it is necessary to consider the stability of the system and the fatigue strength of the cylinder material and the piston rod. In this paper the cylinder is regarded as a slender system. Lech Tomski has developed basic mathematical models of these structures. The first one concerns transverse free vibrations and static stability of a hydraulic cylinder as slender systems [1]. This model was used in the work [2]. The second model concerns the free and forced vibrations of a hydraulic cylinder (a curved system) in the longitudinal direction, which was presented, among others, in the paper [3]. The analysis of the stability of the hydraulic cylinder was undertaken in publications [1, 2, 4-7]. Uzny and Kutrowski [4, 5] studied the telescopic hydraulic cylinder characterized by the number of stages greater than one, limiting themselves to fully extended systems. The paper [2] covers the research on the stiffness of the mountings of a single-stage telescopic hydraulic cylinder. It presents the results of numerical and experimental calculations. A comparison of an approximate model of numerical calculation of stability of a DNV-GL compliant hydraulic cylinder and finite element method is presented in [6]. The effect of manufacturing inaccuracy of hydraulic cylinder components and wear of sealing elements on the stability of the cylinders based on numerical and experimental calculations are presented in [7]. A study based on the large deformation theory and the Timoshenko beam theory of a horizontal hydraulic cylinder articulated on both supports is presented in [8]. A simplified and at the same time practical design constraint for a double acting hydraulic cylinder is presented in publication [9]. Solazzi and Buffoli [10] presented results that show that the hydraulic cylinder made of composite material has a very similar performance, in terms of the safety factor, to the hydraulic cylinder made of structural steel and that the weight reduction is about 87%. The purpose of the research presented in [11] is to evaluate the variability of the buckling load in thin orthotropic cylindrical shells due to the deviation with respect to the nominal values, for geometrical and material properties.

2. Formulation of boundary problem

The considered system is shown in Figure 1. In this paper, the behaviour of a two-stage hydraulic cylinder in its full range of operation is considered. To consider the hydraulic cylinder in its full range of operation, five schemes are considered: A, AB, B, BC, C (Fig. 1) corresponding to five possible stages of its work. The scheme A corresponds to the fully complex hydraulic cylinder. In the hydraulic cylinder corresponding to scheme AB, the second cylinder is extended. Scheme B corresponds to a hydraulic cylinder with the second cylinder fully extended. The stage of the hydraulic cylinder during which the piston rod extends is represented by diagram BC. The fully extended hydraulic cylinder is represented by the last diagram – C. The hydraulic cylinder consists of three components. Two of them are cylinders, and one is the piston rod of the hydraulic cylinder. The tested object is subjected to Euler loading characterized by a constant direction of action when the system is tilted out of the equilibrium position. This direction is consistent with the non-deformed axis of the system.

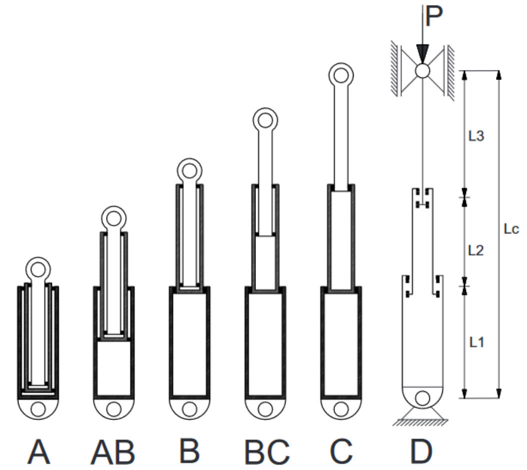

Fig. 1. Schematic of the hydraulic cylinder under consideration: successive stages of hydraulic cylinder extension: A, AB, B, BC, C; mathematical model D

The mathematical model considers the stiffnesses, masses and mass moments of inertia of the sealing and guiding elements occurring between its members. In this paper, a hydraulic cylinder is considered that is articulated at both ends. Figure 2 shows the successive stages of the hydraulic cylinder extension with discrete elements in the form of translational and rotational springs (K and C, respectively). These elements are used to model the guide and seal stiffnesses. In this paper, the bottom cylinder (characterized by the largest diameter) is denoted by the number 1, the top cylinder by the number 2, and the piston rod by the number 3. In order to consider the hydraulic cylinder in its full range of operation, each cylinder element is divided into two parts. The subdivision point of each cylinder element depends on the momentary position of the extended element. The members (after division) with indexes 11 and 12 refer to the lower cylinder; members 21 and 22 correspond to the upper cylinder. Members 31 and 32 correspond to the piston rod. The position of the dividing point in the case of an element which does not extend relative to the adjacent element is not relevant (e.g., the dividing point may be taken at half the length of the element under consideration). For example: in an arrangement according to scheme AB (Fig. 1) in a piston rod numbered 3, the position of the dividing point between the elements 31 and 32 of the piston rod is irrelevant (piston rod 3 does not move relative to cylinder 2). In the arrangement according to scheme BC, in the lower cylinder designated 1, the position of the dividing point between elements 11 and 12 is irrelevant (cylinder 1 does not move relative to cylinder 2). The discrete elements modelling the guiding and sealing systems of the individual cylinder members are designated as follows: C_k^{ij}, K_k^{ij} – the torsional and translational stiffness of the guiding and sealing system, respectively and sealing system, which occurs between the i-th and j-th cylinder member. The upper index k takes the values 0 and 1. The value $k = 0$ corresponds to the lower sealing and guiding system between the i-th and j-th members of the cylinder. The value $k = 1$ is assigned to the upper sealing and guiding arrangement. When the letter *R* appears in the designation, it means that the upper and lower sealing and guiding systems have made contact as a result of the hydraulic cylinder operation. The stiffness containing the designation *R* is therefore the reduced stiffness: $C_R^{ij} = C_0^{ij} + C_1^{ij}$; $K_R^{ij} = K_0^{ij} + K_1^{ij}$. In the same way, the mass *Mu* of the sealing-guiding systems occurring between the individual cylinder members was determined. The masses of the individual sealing-guiding elements were calculated in the following way:

$$Mu_0^{12} = \left(\frac{\pi}{4} \left(\left(d_{w11}\right)^2 - \left(d_{z21}\right)^2 \right) \rho L u_0^{12} \right) \tag{1}$$

$$Mu_0^{23} = \left(\frac{\pi}{4} \left(\left(d_{w21}\right)^2 - \left(d_{T}\right)^2 \right) \rho L u_0^{23} \right) \tag{2}$$

$$Mu_1^{12} = Mu_0^{12};\ Mu_1^{23} = Mu_0^{23} \tag{3}$$

where: Mu_0^{12}, Mu_1^{12} – masses of the sealing-guiding element between cylinder 1 and 2, Mu_0^{23}, Mu_1^{23} – masses of the sealing-guiding element between cylinder 2 and piston-rod 3, Lu_0^{12}, Lu_0^{23} – length of the sealing-guiding elements (Lu_0^{11} = = Lu_1^{32} = $0.05\,L_T$), d_{w21} – internal diameter of cylinder 2, d_{w11} – internal diameter of cylinder 1, d_{z21} – external diameter of cylinder 2, ρ – density of material of the sealing-guiding elements.

The additional letter designation S, in Figure 2, indicates the hydraulic cylinder components transmitting the longitudinal force at a given stage of hydraulic cylinder operation. The dimensions of subsequent components of the cylinder depend on piston rod diameter *dt*, cylinder thickness, thickness g_R and seal thickness g_U. The successive diameters (outer and inner) of individual cylinders can be calculated from the relation:

$$dw_{ij} = dt + 2\left(n-1\right) g_U + 2\left(n - \left(i+1\right)\right) g_R \tag{4}$$

$$dz_{ij} = dt + 2\left(n-i\right) g_U + 2\left(n-i\right) g_R \tag{5}$$

where: $dw_{12} = dw_{11}$, $dw_{22} = dw_{21}$, $dw_{31} = dw_{32}$, $dz_{12} = dz_{11}$, $dz_{22} = dz_{21}$, $dz_{31} = dz_{32}$, g_U and g_R are the thicknesses of sealing-guiding systems and cylinders respectively, *n* – the number of hydraulic cylinder members ($n = 3$), and *i* – stands for the cylinder ($i = 1, 2$).

Each cylinder member is characterized by its bending stiffness $(EI)_{ij}$ and mass per unit length $(\rho A)_{ij}$, respectively. In addition, the mass of the working medium contained in the respective chambers of the cylinders $(\rho A)_{cij}$ is taken into account.

The boundary problem with respect to the natural vibration of the hydraulic cylinder is formulated on the basis of Hamilton's principle.

$$\delta\int_{t1}^{t2}(T-V)\,dt=0 \tag{6}$$

Although the paper considers the full range of operation of the two-stage hydraulic cylinder, the presentation of the boundary problem is limited to the stage of extending the cylinder marked AB. This stage corresponds to the ejection of the first stage of the hydraulic cylinder. The formulation corresponding to the remaining stages of the cylinder is carried out analogically. These formulations are omitted since their complete presentation would significantly increase the volume of this paper. The potential energy V of the considered system in the case of configuration AB can be written in the following form:

$$\begin{aligned}
V=&\sum_{i=1}^{n}\sum_{j=1}^{n}\frac{EI_{ij}}{2}\int_0^{L_{ij}}\left(\frac{\partial^2 Y_{ij}(x_{ij},t)}{\partial x_{ij}^2}\right)^2 dx_{ij}+\\
&-\frac{P}{2}\left[\sum_{i=1}^{2}\int_0^{L_{3i}}\left(\frac{\partial Y_{3i}(x_{3i},t)}{\partial x_{3i}}\right)^2 dx_{3i}+\int_0^{L_{11}}\left(\frac{\partial Y_{11}(x_{11},t)}{\partial x_{11}}\right)^2 dx_{11}\right]+\\
&+\frac{1}{2}C_0^{12}\left(\left.\frac{\partial Y_{11}(x_{11},t)}{\partial x_{11}}\right|^{x_{11}=L_{11}}-\left.\frac{\partial Y_{21}(x_{21},t)}{\partial x_{21}}\right|_{x_{21}=0}\right)^2+\\
&+\frac{1}{2}C_0^{23}\left(\left.\frac{\partial Y_{31}(x_{31},t)}{\partial x_{31}}\right|_{x_{31}=0}-\left.\frac{\partial Y_{21}(x_{21},t)}{\partial x_{21}}\right|_{x_{21}=0}\right)^2+\\
&+\frac{1}{2}C_1^{12}\left(\left.\frac{\partial Y_{12}(x_{12},t)}{\partial x_{12}}\right|^{x_{12}=L_{12}}-\left.\frac{\partial Y_{22}(x_{22},t)}{\partial x_{22}}\right|_{x_{22}=0}\right)^2+\\
&+\frac{1}{2}C_1^{23}\left(\left.\frac{\partial Y_{22}(x_{22},t)}{\partial x_{22}}\right|^{x_{22}=L_{22}}-\left.\frac{\partial Y_{32}(x_{32},t)}{\partial x_{32}}\right|^{x_{32}=L_{32}}\right)^2+\\
&+\frac{1}{2}K_0^{12}\left(Y_{11}\left(L_{11},t\right)-Y_{21}\left(0,t\right)\right)^2+\frac{1}{2}K_0^{23}\left(Y_{31}\left(0,t\right)-Y_{21}\left(0,t\right)\right)^2+\\
&+\frac{1}{2}K_1^{12}\left(Y_{12}\left(L_{12},t\right)-Y_{22}\left(0,t\right)\right)^2+\frac{1}{2}K_1^{23}\left(Y_{22}\left(L_{22},t\right)-Y_{32}\left(L_{32},t\right)\right)^2
\end{aligned} \tag{7}$$

The kinetic energy T of the considered system in the case of configuration AB can be written in the following form:

$$T=\sum_{i=1}^{n}\sum_{j=1}^{n}\frac{(\rho A)_{ij}}{2}\int_{0}^{L_{ij}}\left(\frac{\partial Y_{ij}(x_{ij},t)}{\partial t}\right)^{2}dx_{ij}+\frac{(\rho A)_{c11}}{2}\int_{0}^{L_{11}}\left(\frac{\partial Y_{11}(x_{11},t)}{\partial t}\right)^{2}dx_{11}+$$
$$+\frac{1}{2}Mu_{0}^{12}\left(\left.\frac{\partial Y_{21}(x_{21},t)}{\partial t}\right|_{x_{21}=0}\right)^{2}+\frac{1}{2}Mu_{0}^{23}\left(\left.\frac{\partial Y_{31}(x_{31},t)}{\partial t}\right|_{x_{31}=0}\right)^{2}+$$
$$+\frac{1}{2}Mu_{1}^{12}\left(\left.\frac{\partial Y_{12}(x_{12},t)}{\partial t}\right|^{x_{12}=L_{12}}\right)^{2}+\frac{1}{2}Mu_{1}^{23}\left(\left.\frac{\partial Y_{22}(x_{22},t)}{\partial t}\right|^{x_{22}=L_{22}}\right)^{2}+ \tag{8}$$
$$+\frac{1}{2}Ju_{0}^{11}\left(\left.\frac{\partial^{2} Y_{11}(x_{11},t)}{\partial x_{11}\partial t}\right|_{x_{11}=0}\right)^{2}+\frac{1}{2}Ju_{1}^{32}\left(\left.\frac{\partial^{2} Y_{32}(x_{32},t)}{\partial x_{32}\partial t}\right|^{x_{32}=L_{32}}\right)^{2}$$

where: Ju_0^{11}, Ju_1^{32} – mass inertia moment of lower and upper support of hydraulic cylinder ($Lu_0^{11} = Lu_1^{32} = 0.05\ L_T$):

$$Ju_{0}^{11}=\frac{\pi}{48}\left(\left(d_{z11}\right)^{2}Lu_{0}^{11}\rho\left\{\left(Lu_{0}^{11}\right)^{2}+\frac{3}{4}\left(d_{z11}\right)^{2}\right\}\right) \tag{9}$$

$$Ju_{1}^{32}=\frac{\pi}{48}\left(\left(d_{T}\right)^{2}Lu_{1}^{32}\rho\left\{\left(Lu_{1}^{32}\right)^{2}+\frac{3}{4}\left(d_{T}\right)^{2}\right\}\right) \tag{10}$$

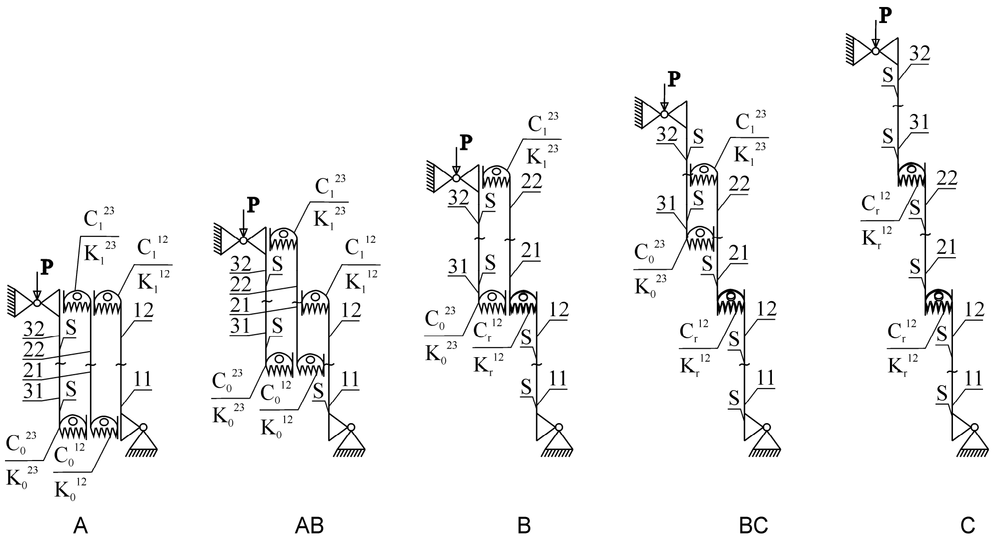

Fig. 2. Mathematical scheme of the considered hydraulic cylinder cases

The member $(\rho A)_{cij}$ written in the kinetic energy equation occurs only in those parts of the cylinders that are filled with the working medium. This paper assumes that the considered hydraulic cylinder is located in the vertical position. In the case of a different orientation in the mathematical model, the initial deflection of the system caused by the force of gravity of these individual elements should be taken into account.

After taking into account the potential and kinetic energy and performing the necessary mathematical transformations, the differential equations of motion of the system and the natural boundary conditions are obtained. The differential equations of motion after taking into account the solution of the form:

$$Y_{ij}\left(x_{ij},t\right)=y_{ij}\left(x_{ij}\right)\cos\left(\omega t\right) \tag{11}$$

can be written as follows:

$$\left(EJ\right)_{ij}\frac{d^4 y_{ij}\left(x_{ij}\right)}{dx_{ij}^4}+P_{ij}\frac{d^2 y_{ij}\left(x_{ij}\right)}{dx_{ij}^2}-\left[\left(\rho A\right)_{ij}+\left(\rho A\right)_{cij}\right]\omega^2 y_{ij}\left(x_{ij}\right)=0 \tag{12}$$

where: $i = 1, 2, 3$; $j = 1, 2$; ω – natural frequency, and $P_{11} = P_{31} = P_{32} = P$; $P_{12} = P_{21} = P_{22} = 0$; $(\rho A)_{c12} = (\rho A)_{c21} = (\rho A)_{c22} = (\rho A)_{c31} = (\rho A)_{c32} = 0$.

In this paper, an example of geometric and natural boundary conditions is presented for the AB scheme (Fig. 2):

$$y_{11}\left(0\right)=y_{32}\left(L_{32}\right)=0;\ y_{i1}\left(L_{i1}\right)=y_{i2}\left(0\right);\ y_{i1}^{I}\left(L_{i1}\right)=y_{i2}^{I}\left(0\right) \tag{13-16}$$

where $i = 1, 2, 3$.

$$(EI)_{11}y_{11}^{III}(L_{11})+Py_{11}^{I}(L_{11})-K_0^{12}\big(y_{11}(L_{11})-y_{21}(0)\big)-(EI)_{12}y_{12}^{III}(0)=0 \tag{17}$$

$$-(EI)_{11}y_{11}^{II}(L_{11})-C_0^{12}\big(y_{11}^{I}(L_{11})-y_{21}^{I}(0)\big)+(EI)_{12}y_{12}^{II}(0)=0 \tag{18}$$

$$(EI)_{31}y_{31}^{III}(L_{31})+Py_{31}^{I}(L_{31})-(EI)_{32}y_{32}^{III}(0)-Py_{32}^{I}(0)=0 \tag{19}$$

$$-(EI)_{31}y_{31}^{II}(L_{31})+(EI)_{32}y_{32}^{II}(0)=0 \tag{20}$$

$$(EI)_{21}y_{21}^{III}(L_{21})-(EI)_{22}y_{22}^{III}(0)+K_1^{12}\big(y_{12}(L_{12})-y_{22}(0)\big)=0 \tag{21}$$

$$-(EI)_{21}y_{21}^{II}(L_{21})+(EI)_{22}y_{22}^{II}(0)+C_1^{12}\big(y_{12}^{I}(L_{12})-y_{22}^{I}(0)\big)=0 \tag{22}$$

$$(EI)_{11}y_{11}^{II}(0)+Ju_0^{11}\omega^2 y_{11}^{I}(0)=0 \tag{23}$$

$$(EI)_{12}y_{12}^{III}(L_{12})+Mu_1^{12}\omega^2 y_{11}(L_{12})-K_1^{12}\big(y_{12}(L_{12})-y_{22}(0)\big)=0 \tag{24}$$

$$-(EI)_{12}y_{12}^{II}(L_{12})+Ju_1^{12}\omega^2 y_{12}^{I}(L_{12})-C_1^{12}\left(y_{12}^{I}(L_{12})-y_{22}^{I}(0)\right)=0 \tag{25}$$

$$\begin{aligned}&(EI)_{21}y_{21}^{III}(0)-Mu_0^{12}\omega^2 y_{21}(0)+K_0^{12}(y_{11}(L_{11})-y_{21}(0))+\\&-K_0^{23}(y_{31}(0)-y_{21}(0))=0\end{aligned} \tag{26}$$

$$\begin{aligned}&(EI)_{21}y_{21}^{II}(0)+Ju_0^{12}\omega^2 y_{21}^{I}(0)-C_0^{12}\left(y_{11}^{I}(L_{11})-y_{21}^{I}(0)\right)+\\&+C_0^{23}\left(y_{31}^{I}(0)-y_{21}^{I}(0)\right)=0\end{aligned} \tag{27}$$

$$(EI)_{22}y_{22}^{III}(L_{22})+Mu_1^{23}\omega^2 y_{22}(L_{22})-K_1^{23}(y_{22}(L_{22})-y_{32}(L_{32}))=0 \tag{28}$$

$$-(EI)_{22}y_{22}^{II}(L_{22})+Ju_1^{23}\omega^2 y_{22}^{I}(L_{22})-C_1^{23}\left(y_{22}^{I}(L_{22})-y_{32}^{I}(L_{32})\right)=0 \tag{29}$$

$$(EI)_{31}y_{31}^{III}(0)+Mu_0^{23}\omega^2 y_{31}(L_{31})-Py_{31}^{I}(0)-K_0^{23}(y_{31}(0)-y_{21}(0))=0 \tag{30}$$

$$(EI)_{31}y_{31}^{II}(0)+Ju_0^{23}\omega^2 y_{31}^{I}(0)-C_0^{23}\left(y_{31}^{I}(0)-y_{21}^{I}(0)\right)=0 \tag{31}$$

$$-(EI)_{32}y_{32}^{II}(L_{32})+Ju_1^{32}\omega^2 y_{32}^{I}(L_{32})+C_1^{23}\left(y_{22}^{I}(L_{22})-y_{32}^{I}(L_{32})\right)=0 \tag{32}$$

The solution of differential equations (10) can be represented as follows:

$$y_{ij}\left(x_{ij}\right)=A_{ij}\cosh\left(\alpha_{ij}x_{ij}\right)+B_{ij}\sinh\left(\alpha_{ij}x_{ij}\right)+C_{ij}\cos\left(\beta_{ij}x_{ij}\right)+D_{ij}\sin\left(\beta_{ij}x_{ij}\right) \tag{33}$$

where:

$$\begin{aligned}&\alpha_{ij}=\sqrt{-\frac{k_{ij}^2}{2}+\sqrt{\frac{k_{ij}^4}{4}+\Omega_{ij}^2}}\,;\ \beta_{ij}=\sqrt{\frac{k_{ij}^2}{2}+\sqrt{\frac{k_{ij}^4}{4}+\Omega_{ij}^2}}\,;\\&\Omega_{ij}^2=\frac{\left((\rho A)_{ij}+(\rho A)_{cij}\right)\omega^2}{(EI)_{ij}};\ k_{ij}^2=\frac{P_{ij}}{(EI)_{ij}}\end{aligned} \tag{34 a-d}$$

The solutions (33) are substituted into the boundary conditions (13-32) to form a system of equations. The determinant of the matrix of coefficients of this system of equations equated to zero is the governing equation by which the critical force and natural frequencies of the system are determined.

3. Results of numerical calculation

This paper presents the results of numerical calculations concerning the influence of seal and guide stiffness on the value of critical force, which can be applied to the tested system in its full range of operation. Characteristic curves (curves in the plane load – natural frequency) for selected degrees of hydraulic cylinder separation are also presented. The cylinder is a system, in the case of which there is a high probability of time-varying forces acting on it. Therefore, it is justified to present the results in the form of characteristic curves. The results are presented in the dimensionless form with use the following quantities:

$$\zeta_{GU} = \frac{g_U}{dt};\ \zeta_{GR} = \frac{g_R}{dt};\ \lambda_{CR} = \frac{PL_t^2}{(EI)_t};\ \Omega = \frac{\omega^2(\rho A)_n L_t^4}{(EI)_t};$$
$$\zeta C_{ij} = \frac{C_{ij}L_t}{(EI)_t};\ \zeta K_{ij} = \frac{K_{ij}L_t^3}{(EI)_t};\ \zeta_L = \frac{L_c}{L_t} \tag{35}$$

where: ζ_{GU} – thickness parameter of sealing and guiding systems, ζ_{GR} – cylinder thickness parameter, λ – external load parameter, Ω – natural frequency parameter, $(EI)_t$ – bending stiffness of the piston rod, L_t – length of the piston rod, ζC_{ij}, ζK_{ij} – stiffness parameter of the rotational and translational springs respectively, ζ_L – pitch parameter of the hydraulic cylinder, L_c – actual length of the hydraulic cylinder.

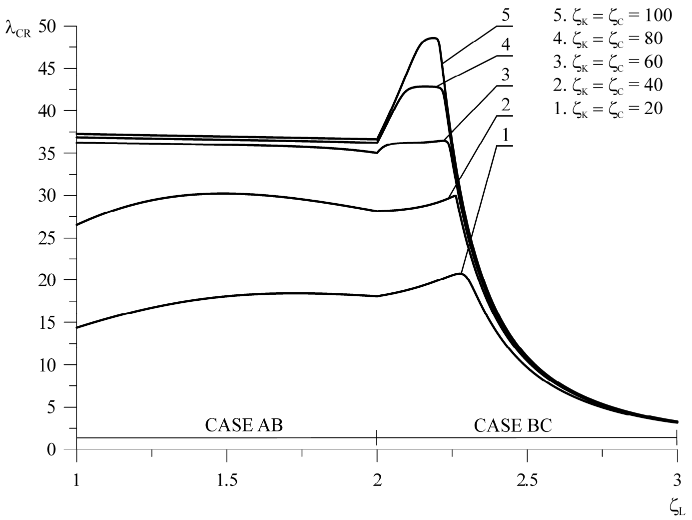

Fig. 3. Diagram of the critical force value as a function of the current actuator length parameter

Figure 3 shows the critical load parameter depending on the hydraulic cylinder extension ratio parameter. The calculations were carried out for five stiffnesses of sealing and guiding systems located between successive hydraulic cylinder members ($\zeta_C = \zeta_K = 20$; $\zeta_C = \zeta_K = 40$; $\zeta_C = \zeta_K = 60$; $\zeta_C = \zeta_K = 80$; $\zeta_C = \zeta_K = 100$). Equal values of parameters determining translational and rotational stiffnesses of sealing-guiding systems were assumed in the calculations.

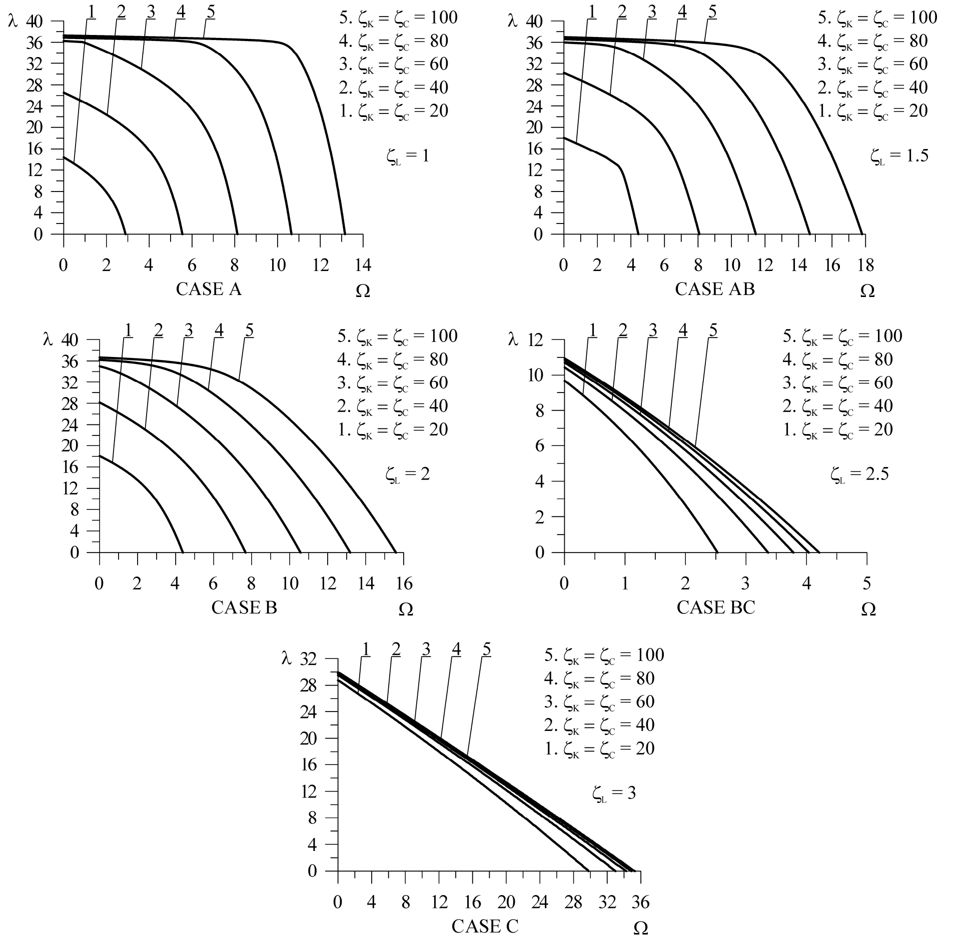

Fig. 3 a-e. Characteristic curves in the plane of the load parameter λ – the first natural frequency parameter at different parameter values ζC_{ij}, ζK_{ij}

It was additionally assumed that considered stiffnesses between all cylinder members are also equal. In the case when $\zeta_C = \zeta_K = 20$ and 40, there is a slight increase in the critical force during the initial phase of the first stage until the maximum value is reached. Then, the critical force decreases. It reaches its lowest value when the stage is fully extended (the phase of the hydraulic cylinder operation corresponding to the diagram B – Fig. 2). If $C = K = 60$; 80; 100 the change of the critical load while extending the first stage is small. The small change of the critical load in this phase of the cylinder operation is caused by the fact that its value depends on the stability of the piston rod. The critical load increases and then decreases during piston rod advance (the working phase modelled by the BC scheme – Fig. 2). The lowest value of the critical load occurs in the case of the fully extended piston rod. The influence of stiffness of the sealing-guiding systems on the critical load of the fully extended hydraulic cylinder is small. The magnitude and dynamics of the critical load increase in the first stage of piston rod advance depends on the stiffness of the sealing-guiding systems under consideration. The increase of the critical load is caused by the shortening of the buckling length of the piston rod, which has a significant influence on the stability of the whole system up to a certain stage of the hydraulic cylinder extension. Figure 4 shows the characteristic curves that were determined at different stages of cylinder operation (ζ_L = 1, 1.5, 2, 2.5, 3). Geometric parameters of the hydraulic cylinder under consideration: piston rod diameter – $dt = 0.02$ m, thickness of sealing and guiding systems – $\zeta_{GU} = \zeta_{GR} = 0.5$.

The natural frequency increases with the increase in the stiffness of the sealing and guiding systems in all presented stages of the hydraulic cylinder operation. The magnitude of this increase depends on the extension of the hydraulic cylinder. The smallest effect of stiffnesses C and K on the frequency is obtained when the hydraulic cylinder is fully extended (scheme C), and the largest when the hydraulic cylinder is retracted (scheme A). At higher stiffnesses K and C, at certain stages of the hydraulic cylinder operation, a rapid decrease in natural frequency can be observed at external loads close to the critical load. This rapid decrease in frequency occurs at the initial stage of hydraulic cylinder extension. The greater the degree of extension of the cylinder (higher value of the L parameter), the shorter the fragment of the characteristic curves corresponding to the rapid frequency drop.

4. Conclusions

In this paper, the boundary problem of a telescopic hydraulic cylinder subjected to Euler loading is considered. The boundary problem was formulated on the basis of Hamilton's principle. Based on the mathematical model, numerical calculations were carried out. The value of critical force that can be loaded on the hydraulic cylinder during its operation was determined. The results of numerical calculations were presented as a dimensionless critical force parameter depending on the current length of the hydraulic cylinder. Additionally, characteristic curves on the plane: the parameter of external – the parameter of the first natural frequency were presented. Numerical calculations were carried out in the direction of the influence of the stiffness of the sealing-guiding systems and the degree of hydraulic cylinder extension on the critical load and the relation between the natural frequency and the external load.

In this paper, only the strength aspect of the hydraulic cylinder was considered, consisting in the study of stability (determination of critical load). In a real hydraulic cylinder, the strength of the cylinder, apart from buckling, depends on the strain of the cylinder material caused by high working pressure. Therefore, the formulation of the stability problem presented here should be supplemented with the strength of cylinders and sealing elements in subsequent works in the considered field.

References

[1] Tomski, L. (1977). Elastic carrying capacity of a hydraulic prop. *Engineering Transactions*, *25*(20), 247-263.

[2] Uzny, S. (2009). Free vibrations and stability of hydraulic cylinder fixed elasically on both ends. *Proc. Appl. Math. Mech.*, *9*, 303-304.

[3] Tomski, L. (1979). Dynamika stojaków hydraulicznych obudów górniczych, Praca habilitacyj-na, Nr 17, Częstochowa.

[4] Uzny, S., & Kutrowski, Ł. (2018). The effect of the type of mounting on stability of a hydraulic telescopic cylinder. *Machine Dynamics Research*, *42*(2), 53-60.

[5] Uzny, S., & Kutrowski, Ł. (2018). Obciążalność rozsuniętego teleskopowego siłownika hydrau-licznego przy uwzględnieniu wyboczenia oraz wytężenia materiału. *Modelowanie Inżynierskie*, *37*(68), 125-131.

[6] Narvydas, E. (2016). Buckling strength of hydraulic cylinders – and engineering approach and finite element analysis. *Mechanika*, *22*(6), 474-477.

[7] Gamez-Montero, P.J., Salazar E., Castilla R., Freire J., Khamashta M., & Codina E. (2009). Misalignment effects on the load capacity of a hydraulic cylinder. *International Journal of Mechanical Sciences*, *51*(2), 105-113.

[8] Ji, Zhou, Duanwei, Shi, Chengyun, Di, Yang, Zhang, & Xionghao, Cheng (2020). Buckling behavior of horizontal hydraulic cylinder articulated at both supports. *International Journal of Structural Stability and Dynamics, 20*(3), 2050033.

[9] Zhang, X., Zhang, J., Cheng, M., Zheng, S., Xu, B., & Fang, Y. (2022). A design constraint for a double-acting telescopic hydraulic cylinder in a hydraulic erecting system. *Journal of Zhejiang University-SCIENCE A (Applied Physics & Engineering)*, *23*(1),1-13.

[10] Solazzi, L., & Buffoli, A. (2021). Fatigue design of hydraulic cylinder made of composite mate-rial. *Composite Structures*, *277*, 114647.

[11] Solazzi, L. (2022). Reliability evaluation of critical local buckling load on the thin walled cylin-dricall shell made of composite material. *Composite Structures, 284*, 115163.